Response to the co-editor on SEAC4RS OT manuscript acp-2016-1065.

Dear co-editor and staff,

We thank the co-editor and two reviewers for very helpful comments and constructive revision requests. We have responded to all comments and minor revision requests as listed below.

Response to co-editor:

Editor's comment 1: There was also a comparison of hygrometers during the NASA MACPEX mission; this study might also be helpful here: Rollins, A. W., et al. (2014).

Author's response to comment 1 and change in manuscript:
The Rollins et al (2014) paper puts these measurements into perspective, namely level of agreement between JLH and Harvard Water Vapor, so we have cited this paper in the text at line 121-122:
"This is consistent with the AquaVIT laboratory intercomparison (Fahey et al., 2014) and other aircraft field missions (e.g., Rollins et al., 2014)."

New reference:
Rollins, A., Thornberry, T., Gao, R. S., Smith, J. B., Sayres, D. S., Sargent, M. R., Schiller, C., Krämer, M., Spelten, N., Hurst, D. F., Jordan, A. F., Hall, E. G., Vömel, H., Diskin, G. S., Podolske, J. R., Christensen, L. E., Rosenlof, K. H., Jensen, E. J., and Fa- hey, D. W.: Evaluation of UT/LS hygrometer accuracy by inter- comparison during the NASA MACPEX mission, J. Geophys. Res.-Atmos., 119, doi:10.1002/2013JD020817, 2014.

Editor's comment 2: Tissier and Legras also discuss the accuracy of the OT altitude and obtain a somewhat different result than reported here (l. 169)

Author's response to comment 2:
We assume that the editor is referring to the following comment made in Tissier and Legras: "We use the CLAUS data set (Hodges et al., 2000), which provides global 3-hourly maps of brightness temperature at 30km resolution, combined with ERA-Interim data (Dee et al., 2011) to determine the pressure of the top of the convective clouds.....This method is, however, limited by the inability to distinguish overlaying cirrus from convective tops and is known to underestimate the altitude of the deep convective clouds by about 1 km (Sherwood et al., 2004; Minnis et al., 2008)."

The editor is correct in that, in situations with above anvil cirrus plumes (i.e. “overlaying cirrus from convective tops”) described by Setvak et al in numerous papers and Homeyer (JAS, 2014) and et al. (JAS, 2017), the IR brightness temperature (BT) in these plumes is anomalously warm because the cirrus adjusts to the stratospheric temperature warmer than the tropospheric primary anvil cloud. If one matches the warm IR BT to a sounding and only considers to height assign the cloud to the troposphere, then yes there will be a low bias in cirrus plume heights. Above anvil cirrus only occurs with a small subset of all overshooting convection though. We are looking at convective cores that generate the plumes due to favorable wind shear inducing gravity wave breaking. Cores (i.e. OTs) are significantly colder than the surrounding anvil, and the Griffin et al approach is based on this premise. So, the editor’s comment about a discrepancy in height assignment errors is not an “apples to apples” comparison of phenomena and thus is not relevant to our paper or results.

<u>Editor's comment 3:</u> The authors argue on the efficiency of mixing by breaking gravity waves (l. 188 and l. 296). Please consider this citation from a review of another paper (review by T. Dunkerton):
“..vertical diffusion to breaking gravity waves, it is well-known that such waves (if undergoing local convective instability in their phase of overturning) are not effective in mixing heat and constituents vertically (Coy et al., 1988 JAS). Inertia-gravity waves may undergo shear instability at large amplitude, altering this result possibly in a significant way (Dunkerton, 1985 JAS, et seq.). “

<u>Author's response to comment 3:</u>
In our manuscript (line 188), we cite recent references in the literature: "turbulent processes such as gravity wave breaking mix tropospheric and stratospheric air (e.g., Mullendore et al., 2009, 2005; Wang 2003; Homeyer et al. 2017).”
With regards to the Dunkerton comment, Homeyer et al (2017) and Wang (2003) clearly show water vapor enhancement in the stratosphere due to these waves. Perhaps Dunkerton’s findings seemed robust at the time, but advancements in satellite imagery and modeling capabilities have since highlighted the importance of these waves for generating the detrainment and irreversible mixing of ice (and thus water vapor via sublimation) in the stratosphere.

<u>Editor's comment 4:</u> l.257: I find this sentence confusing, please consider to rephrase.

“This case is an example of the classic North American Monsoon circulation with a moisture source over the Sierra Madre Occidental. Anticyclonic transport carried the moisture north from Mexico, and counter-clockwise around the high pressure (Figure 8b).”

Author's response to comment 4 and change in manuscript:
The editor is correct that this wording is confusing. Figure 8b shows the dominant anticyclonic transport of the North American Monsoon. We have reworded and merged the two sentences as follows:
“This case is an example of the classic North American Monsoon circulation with a moisture source over the Sierra Madre Occidental (Adams and Comrie, 1997), in which air parcels are transported from OT in Mexico, around the anticyclone, to the CONUS (Figure 8b).”

New reference:
Adams, D. K., and A. C. Comrie, 1997: The North American Monsoon. *Bull. Amer. Meteor. Soc.*, 78, 2197–2213, doi:http://dx.doi.org/10.1175/JCLI4071.1.

Response to Report #1
This is our response to the minor comments from referee #1:

Referee’s Comment 1:
First, I would find it a lot more informative to combine Figures 2 and 3 to visually compare the mixing ratio distributions below and above 400K. The y-axis would need to be changed to “fraction of observations” by dividing each histogram by the number of observations it contains. In other words, the sum of fractions within each histogram would be unity.

Author’s response to comment 1 and changes to manuscript:
We agree with referee #1 that it would be good to combine Figures 2 and 3. The new Figure 2 in the revised manuscript combines these two histograms, y-axis changed to “fraction of observations” and data normalized to the number of observations.

Referee’s Comment 2:
Second, with the introduction of Figure 10 there now exists a real contradiction in the paper. Figure 10 implies that, on average, about 50% of the air masses sampled

between 370 and 420K during the three studied flights were connected to convective overshooting tops. This is in stark contrast to the 5% of air masses sampled between 370 and 420K that had "enhanced water". I think the problem lies in the very high (9.7 ppmv) threshold for enhanced water in the 380-400K layer. From Figure 2 the distribution of mixing ratios is skewed to higher values and is quite non-Gaussian. Thus, the choice of mean + 2*stddev as the threshold yields a very high value. I would be tempted to try a different a different statistic, perhaps involving the median of the highly skewed distribution, to calculate a threshold. I realize this threshold is subjectively determined, but the contradiction the current threshold creates leaves the reader somewhat perplexed: Why aren't 50% of the measurements considered "enhanced water" when 50% of the air masses were connected to OTs? Don't be concerned that the enhanced water fraction from the JLH measurements is much higher than that from MLS because the three SEAC4RS flights were targeting air masses influenced by convection. And to avoid any mis-interpretation of 50% enhanced water and Figure 10 (as supporting Anderson et al. 2012) I would make sure to clearly state that the three SEAC4RS flights targeted air masses influenced by convection.

<u>Author's response to Comment 2:</u>
We appreciate this excellent comment by the reviewer.
In this manuscript, we **conservatively** defined "enhanced water" as mean + 2*stddev to exclude the larger population of measurements at 6 to 9.7 ppmv water vapor that may have other sources. Figures 1 and 2 show the statistics of the entire ensemble of 23 aircraft flights, some of which did not target air masses influenced by convection. Thus, the Figure 2 distribution shows only a small fraction of CONUS air parcels with "enhanced water." Figure 10 shows only three flights, the case studies, with 50% "enhanced water."
This apparent contradiction is resolved by a new statement to be added that the three SEAC4RS flights in Figure 10 (now renumbered to Figure 9) deliberately targeted air masses influenced by convection. Therefore the fraction of mass masses influenced by convective OT is higher than for the entire CONUS.

<u>Author's change in manuscript in response to Comment 2:</u>
The new text at lines 281 to 285 is:
"For all the back trajectories in the three case studies, the fraction that connect to OT within the previous seven days ranges from 30% to 70% (Figure 9). The three aircraft flight dates analyzed in Figure 9 have a higher fraction of enhanced water than the other flights. These three flights deliberately targeted air masses

influenced by convection. For the CONUS in general, the fraction of air parcels at 370-420 K influenced by OT is much smaller.”

Response to Report #2

Referee #2 says that "the authors have significantly improved the manuscript. Together with the changes made in response to the first reviewer, the authors have addressed all my concerns."

We thank referee #2, and have completed all Technical corrections recommended by referee #2:

Line 23: Better write: ‘… satellite infrared window-channel brightness-temperature gradients …’ (note the hyphens).
Done.

Line 111: ‘H2O is 6.7’ (delete for)
Done.

Line 111: ‘Thus, …‘ (added comma)
Done.

Line 152: ‘Data for’ (not From)
Done.

Line 197: which should it be: ‘storm-updraft tracks’ or ‘storm updraft-tracks’?
Changed to "tracks of storm updrafts"

Line 212: delete ‘also’
Done.

Line 274: ‘In this paper, …’
Done.

Line 276: duplicate ‘initialized’
Done.

Figure 4: Please remove grey background.

Done.

Title

Enhanced Stratospheric Water Vapor over the Summertime Continental United States and the Role of Overshooting Convection

Robert L. Herman[1], Eric A. Ray[2], Karen H. Rosenlof[2], Kristopher M. Bedka[3], Michael J. Schwartz[1], William G. Read[1], Robert F. Troy[1], Keith Chin[1], Lance E. Christensen[1], Dejian Fu[1], Robert A. Stachnik[1], T. Paul Bui[4], Jonathan M. Dean-Day[5]

[1]Jet Propulsion Laboratory, California Institute of Technology, Pasadena, California, USA.

[2]National Oceanic and Atmospheric Administration (NOAA) Earth System Research Laboratory (ESRL) Chemical Sciences Division, Boulder, Colorado, USA.

[3]NASA Langley Research Center, Hampton, Virginia, USA.

[4]NASA Ames Research Center, Moffett Field, California, USA.

[5]Bay Area Environmental Research Institute, Sonoma, California, USA.

Correspondence to: R. L. Herman (Robert.L.Herman@jpl.nasa.gov)

Abstract

The NASA ER-2 aircraft sampled the lower stratosphere over North America during the NASA Studies of Emissions and Atmospheric Composition, Clouds and Climate Coupling by Regional Surveys (SEAC^{4}RS) field mission. This study reports observations of convectively-influenced air parcels with enhanced water vapor in the overworld stratosphere over the summertime continental United States, and investigates in detail three case studies. Water vapor mixing ratios greater than 10 ppmv, much higher than the background 4 to 6 ppmv of the overworld stratosphere, were measured by the JPL Laser Hygrometer (JLH Mark2) at altitudes between 16.0 and 17.5 km (potential temperatures of approximately 380 K to 410 K). Overshooting cloud tops (OT) are identified from a SEAC^{4}RS OT detection product based on satellite infrared window-channel brightness-temperature gradients. Through trajectory analysis, we make the connection between these *in situ* water measurements and OT. Back trajectory analysis ties enhanced water to OT one to seven days prior to the intercept by the aircraft. The trajectory paths are dominated by the North American Monsoon (NAM) anticyclonic circulation. This connection suggests that ice is convectively transported to the overworld stratosphere in OT events and subsequently sublimated; such events may irreversibly enhance stratospheric water vapor in the summer over Mexico and the United States. Regional context is provided by water observations from the Aura Microwave Limb Sounder (MLS).

Deleted:

Deleted:

Keywords

Convection, overshoot, atmospheric water, stratosphere-troposphere exchange

Copyright Statement

Copyright 2017. All rights reserved.

1. Introduction

Water plays a predominant role in the radiative balance of the Earth's atmosphere, both in the gas phase as the Earth's primary greenhouse gas and in condensed phases in cloud and aerosol. Despite its low abundance, upper tropospheric and lower stratospheric (UTLS) water vapor is critically important in controlling outgoing long-wave radiation, and quantifying UTLS water vapor and its controlling processes is critical for climate characterization and prediction. Climate models are sensitive to changes in stratospheric water (Shindell, 2001) and clouds (Boucher et al., 2013). Increases in UTLS water are associated with warming at the surface on the decadal scale (Solomon et al., 2010). As the dominant source of hydroxyl radicals, UTLS water also plays an important role in control of UTLS ozone (Shindell, 2001; Kirk-Davidoff et al., 1999).

The overworld stratosphere, the altitude region with potential temperature θ greater than 380 K (Holton et al. 1995), is extremely dry, with typical mixing ratios of 3—6 parts per million by volume (ppmv). The importance of low temperatures at the tropical tropopause acting as a "cold trap" to prevent tropospheric water from entering the stratosphere has been recognized since Brewer (1949). Tropospheric air slowly ascends through the tropical tropopause layer (TTL) as part of the hemispheric-scale Brewer-Dobson circulation. In the TTL, air passes through extremely cold regions where water vapor condenses in situ to form cirrus ice, and then the cirrus slowly falls due to sedimentation (e.g., Jensen et al., 2013). Additional condensation and sedimentation are thought to be associated with convection and large-scale waves (e.g., Voemel et al., 2002). The amount of water that enters the stratosphere is largely a function of the coldest temperature a parcel trajectory encounters. This typically occurs in the tropics, and the coldest temperature is typically near the tropical tropopause. The saturation mixing ratio at the cold point tropopause thereby sets the entry value of water vapor.

In contrast to water entry into the overworld stratosphere, water transport from the troposphere to the lowermost stratosphere (350 K < θ < 380 K over summer CONUS) may occur through several different pathways. Poleward of the subtropical jet, water may be transported into the lowermost stratosphere through isentropic troposphere-stratosphere exchange (Holton et al., 1995) or through convective overshoot of the local tropopause (Dessler et al., 2007; Hanisco et al., 2007). Isentropic transport from the tropics is the dominant pathway for water into the lowermost stratosphere, with evidence from the seasonal cycle of lower stratospheric water (e.g., Flury et al., 2013). How important sublimation of ice from convective overshoot is for hydrating the stratosphere is a topic of ongoing debate (e.g., Randel et al., 2015; Wang, 2003). Case studies have reported extreme events in which ice is transported to the overworld stratosphere and subsequently sublimates, but the amount of ice that is irreversibly injected into the stratosphere is poorly known. Airborne measurements have demonstrated that convective injection occurs both in the tropics (Webster and Heymsfield, 2003; Corti et al., 2008; Sayres et al., 2010; Sargent et al., 2014) and at mid-latitudes (Hanisco et al., 2007; Anderson et al., 2012). Ice injected directly into the stratosphere is unaffected by the cold trap in the vicinity of the tropopause (Ravishankara, 2012).

The subject of this paper is the role of convective overshooting tops in enhancing stratospheric water. Paraphrasing Bedka et al. (2010), a convective overshooting top (OT) is a protrusion above a cumulonimbus anvil due to strong updrafts above the equilibrium level. Early observations of OT include photographs of OT in the stratosphere from a U-2 aircraft (Roach 1967). Recent observations of elevated water mixing ratios in the summer overworld stratosphere by aircraft (Anderson et al., 2012) and the Aura Microwave Limb Sounder (MLS) (Schwartz et al., 2013) suggest that ice injection into the overworld stratosphere by OT, while rare, occurs in three predominant regions during the summer season. These three regions are the Asian Monsoon region, the South American continent, and – the focus of this study - the North American Monsoon (NAM) region (Schwartz et al., 2013).

The NASA ER-2 aircraft sampled the summer stratospheric NAM region during the NASA Studies of Emissions and Atmospheric Composition, Clouds and Climate Coupling by Regional Surveys (SEAC^{4}RS) field mission (Toon et al., 2016). One of the primary goals of this multi-aircraft mission was to address the question: do deep convective cloud systems locally inject water vapor and other chemicals into the overworld stratosphere over the continental United States (CONUS)? It is challenging for space- and ground-based techniques to detect enhanced water vapor injected into the stratosphere by OT. Satellite measurements are limited by their horizontal and vertical resolution in detecting fine-scale three-dimensional variations in water vapor, while ground-based measurements are confined to sampling at fixed locations. In contrast, airborne *in situ* stratospheric measurements of water have an advantage because the aircraft can be routed to a specific location, altitude, date and time. Modelers can predict whether air parcels are likely to have convective influence, and aircraft flight paths are planned to intercept those air parcels. The purpose of this paper is to report three new case studies of enhanced water vapor in the overworld stratosphere during the NASA SEAC^{4}RS field mission, and to connect these observations to deep convective OT over the North American continent.

2. Observations

2.1 Aircraft

The airborne *in situ* water vapor measurements reported here are from the Jet Propulsion Laboratory Laser Hygrometer Mark2 (JLH Mark2), a tunable laser spectrometer with an open-path cell external to the aircraft fuselage (May, 1998). Water vapor is reported at 1 Hz (10% accuracy), although the time response of the open-path cell is much faster than this because the instrument is sampling the free-stream airflow. This instrument has a redesigned optomechanical structure for greater optical stability, and was first flown in this configuration on the NASA ER-2 high-altitude aircraft during the SEAC^{4}RS field mission. Pressure and temperature, provided by the Meteorological Measurement System (MMS) (Scott et al., 1990), are used in the data processing to calculate water vapor mixing ratios from spectra, as described in May (1998).

During SEAC^{4}RS, nine aircraft flights targeted air parcels with recent convective influence (see Table 3 of Toon et al., 2016). Figure 1 shows the combined vertical profiles of JLH Mark2 water vapor from all 23 SEAC^{4}RS flights. Outliers with high water vapor mixing ratios are the focus on this study. Enhanced water vapor was measured on eleven flights (Table 1). Here we define ‘enhanced water vapor’ as mixing ratios greater than two standard deviations above the mean in situ measurement. For the overworld stratosphere in all 23 SEAC^{4}RS flights, mean

H_2O is 6.7±1.5 ppmv at 380-400 K and 5.0±0.8 ppmv at 400-420 K (Figure 2). Thus, the threshold for enhanced water vapor is 9.7 ppmv at 380-400 K, and 6.6 ppmv at 400-420 K. The majority of measurements have background water mixing ratios characteristic of the overworld stratosphere, 4 to 6 ppmv. In the overworld stratosphere (potential temperature greater than 380 K), Figure 1 shows enhanced water vapor at potential temperatures up to approximately 410 K (17.5 km altitude). We define the 'enhanced water region' as the layer of the overworld stratosphere where these events have been observed, 380-410 K potential temperature corresponding to 16-17.5 km altitude. Enhanced water vapor measured *in situ* by both the JLH Mark2 instrument (Figure 1) and the Harvard Water Vapor instrument (J. B. Smith, pers. comm.) on the NASA ER-2 aircraft indicated that the aircraft intercepted convectively-influenced air. Other tracers measured on the aircraft did not change significantly in these plumes. For the SEAC^{4}RS flights, the agreement between these two water vapor instruments is within +/-10% for stratospheric water. This is consistent with the AquaVIT laboratory intercomparison (Fahey et al., 2014) and other aircraft field missions (e.g., Rollins et al., 2014). The largest enhancements were observed on three flights that are described in detail in Sect. 4.

Deleted: for
Deleted: (Figure 2),
Deleted: 3

2.2 Aura MLS

Aura MLS measures ~3500 profiles each day of water vapor and other atmospheric species (Livesey et al., 2016). While the aircraft samples *in situ* water in a thin trajectory through the atmosphere, Aura MLS provides a larger scale context. Expanding on the analysis of Schwartz et al. (2013), Aura MLS observations of stratospheric water vapor are presented here for the SEAC^{4}RS time period of summer 2013. Aura MLS H_2O has 0.4 ppmv precision at 100 hPa for individual profile measurements, with spatial representativeness of 200 km along line-of-sight (Schwartz et al., 2013). Results shown here use MLS version 4.2 data, but are not significantly different from the previous version 3.3. MLS observations over CONUS are at ~14:10 local time (ascending orbit) and~1:20 local time (descending orbit), with successive swaths separated by ~1650 km. Vertical resolution of the water vapor product is ~3 km in the lower stratosphere (Livesey et al., 2016).

Aura MLS shows a seasonal maximum in water vapor over CONUS in July and August. The histogram of Aura MLS water vapor in Figure 3 indicates that the July-August 2013 CONUS lower stratosphere was drier than the previous nine-summer MLS record (2004 to 2012). Nevertheless, enhanced lower stratospheric water vapor was observed by MLS in 2013 as rare but detectable events. From the MLS histogram, the frequency of 100-hPa H_2O > 8ppmv was 0.9% of the observations in July-August 2013 in the blue shaded box. Figure 4 shows that, out of all MLS 100-hPa water vapor retrievals over the two-month period July to August 2013, water greater than 8 ppmv was measured only nine times over North America (in the blue shaded box), three times near the west coast of Mexico, and once over the Caribbean Sea.

Deleted: Figure 4
Deleted: Figure 5

3. Analysis

Here we briefly describe the analytical technique used to determine whether back trajectories from the aircraft location intersect OT as identified by a satellite OT data product.

3.1 Detection of overshooting tops

In order to link the stratospheric water vapor encountered by the aircraft to the storm systems from which they may have originated, it is necessary to have a comprehensive continental scale catalog of deep convection. Geostationary Operational Environmental Satellite (GOES) infrared imagery is used to assemble a catalog of OTs throughout the U.S. and offshore waters. This catalog was acquired from the NASA LaRC Airborne Science Data for Atmospheric Composition data archive (http://www-air.larc.nasa.gov/cgi-bin/ArcView/seac4rs). Because OTs are correlated with storm intensity, the OT product was primarily developed to benefit the aviation community for more accurate turbulence prediction, as well as the general public for earlier severe storm warnings. However, the product is also ideally suited for identifying storm systems that can moisten the stratosphere.

Deleted: From

Infrared brightness temperatures are used to detect cloud top temperature anomalies within thunderstorm anvils. OT candidates are colder than the mean surrounding anvil, with the temperature difference indicative of both the strength of the convective updraft and the depth of penetration. For a description of the method, the reader is directed to Bedka et al. (2010). The horizontal spatial resolution of the OT product is dependent on the underlying satellite imagery resolution, i.e., the size of the GOES IR pixel, which is 7 km or less over the CONUS. Additional validation of OTs requires comparison with the Global Forecast System (GFS) Numerical Weather Prediction (NWP) model tropopause temperature. The maximum OT cloud height was derived based on knowledge of the 1) OT-anvil temperature difference, 2) the anvil cloud height based on a match of the anvil mean temperature near to the OT and the GFS NWP temperature profile, and 3) a temperature lapse rate within the UTLS region based on a GOES-derived OT-anvil temperature difference and NASA CloudSat OT-anvil height difference for a sample of direct CloudSat OT overpasses (Griffin et al., 2016). Griffin et al. (2016) finds that 75% of OT height retrievals are within 0.5 km of CloudSat OT height, so we conservatively estimate the accuracy of the OT altitude to 0.5 km. For SEAC^{4}RS, every available GOES-East and GOES-West scan (typically 15 min resolution) was processed for the full duration of the mission, even for the non-flight days, yielding a detailed and comprehensive picture of the location, timing, and depth of penetration of convective storms over the entire CONUS. The output files include the OT coordinates, time, overshooting intensity in degrees K – which is related to the temperature difference between the OT and the anvil – and an estimate of maximum cloud height for OT pixels in meters.

The ability of GOES-East and GOES-West to observe an OT depends on its lifetime. OTs are transient events with lifetimes typically less than 30 minutes but can exceed an hour in well-organized storms such as mesoscale convective systems and supercell storms (Bedka et al. 2015; Solomon et al., 2016, and references therein). Animations such as the following show the variability of OTs sampled by GOES at 1-min resolution,

Infrared wavelength animation:

http://cimss.ssec.wisc.edu/goes/srsor2015/800x800_AGOES14_B4_MS_AL_IR_animated_2015222_191500_182_2015223_131500_182_IR4AVHRR2.mp4

Visible wavelength animation:

http://cimss.ssec.wisc.edu/goes/blog/wp-content/uploads/2015/08/150811_goes14_visible_srsor_MS_mcs_anim.gif
It is clear that some OTs are quite persistent and are both prominent and detectable in IR imagery, but the majority of OTs in these particular animations are short lived (< 10 minutes). Within these OTs, strong convective updrafts can transport ice to 16-18 km altitude where turbulent processes such as gravity wave breaking mix tropospheric and stratospheric air (e.g., Mullendore et al., 2009, 2005; Wang 2003; Homeyer et al. 2017), enabling detrainment of ice and stratospheric hydration.

Bedka et al. (2010) showed that the OT detection algorithm has a false positive rate of 4.2% to 38.8%, depending on the size of the overshooting and algorithm settings. As noted above, OTs are transient and can evolve quite rapidly. The storm top characteristics and evolution we see in the GOES data featured in this paper only capture a subset of the storm lifetimes, even if we were to have a 100% OT detection rate, due to the 15 min resolution of the GOES imager. In addition, relatively coarse GOES spatial resolution (up to 7 km over northern latitudes of the US) can cause the Bedka et al. (2010) method to miss some small diameter and/or weak OT regions. We would be able to better map tracks of storm updrafts using data at 1-minute frequency like that shown by Bedka et al. (2015), but this data is not available over broad geographic domains required for our analysis. Given uncertainties in back trajectories, GOES under-sampling, and that many OTs can be located in close proximity to one another, we are not able to make a direct connection between an individual OT and a stratospheric water vapor plume observed a day or more later. Rather, our analysis identifies a cluster of storms that are the best candidates for generating ice that sublimates into enhanced water vapor plumes sampled by the ER-2.

Deleted: storm updraft

3.2 Back trajectory modeling

Back trajectories were run from each flight profile where enhanced water vapor was measured to determine whether the sampled air was convectively influenced. The trajectories were run with the FLEXPART model (Stohl et al., 2005) using NCEP Climate Forecast System version 2 (CFSv2) meteorology (Saha et al., 2014), and the trajectory time step interval was one hour. Trajectories were initialized every second along the flight track profiles and run backward for seven days. A sampled air parcel was determined to be convectively influenced if the back trajectory from that parcel intercepted an OT region. The tolerances for a trajectory to be considered to have intercepted an OT cloud were +/-0.25 degrees latitude and longitude, +/-3 hours, +/-0.5 km in altitude. These tolerances were chosen primarily due to the resolution of the NCEP meteorology used to run the trajectories (1 deg x 1 deg) and based on personal communication with Leonard Pfister.

Deleted: also

4. Case Studies

In this section, we highlight three NASA ER-2 flights where elevated stratospheric water was observed by JLH Mark2. These dates are 8, 16 and 27 August 2013. Similar results are seen from other hygrometers on the NASA ER-2 aircraft (J. B. Smith, pers. comm.). For each of these ER-2 flights, the back trajectories are presented along with the intersection of coincident OT. The cases are described below.

4.1 First case: 8 August 2013

Figure 5 shows details of the 8 August 2013 ER-2 aircraft flight. This flight was the transit flight from Palmdale, California (34.6 °N, 118.1 °W), to Ellington Field, Houston, Texas (29.6 °N, 95.2 °W). In addition to sending the NASA ER-2 aircraft to the destination base, the science goal of this flight was to profile the North American Monsoon region with five profiles plus the aircraft ascent and final descent. This flight shows a dramatic transition from west to east of background stratospheric water to enhanced water. In the lowermost stratosphere (350 K < θ < 380 K), water can be highly variable, but at 90 hPa it is generally unusual to observe water vapor greater than 6 ppmv. As shown in Figure 5c, there is a gradient in water vapor from west to east: 4.0 to 4.4 ppmv at 90 hPa (17 km) over the west coast of CONUS (black and blue points), and greater than 10 ppmv at 90 hPa over Texas (green points). Simultaneous Aura MLS retrievals also demonstrate a west-to-east water vapor gradient on this day (lines and filled circles in Figure 5c). Both JLH Mark2 and Aura MLS water vapor exceed the thresholds for enhanced water vapor.

Deleted: Figure 6

Deleted: Figure 6

Deleted: Figure 6

Analysis of the 8 August 2013 case is shown in Figure 6. For clarity only some example trajectories (a subset of our analysis) are shown. These are displayed as thin blue traces in panels (b) and (c). The intersections of the example trajectories with coincident OT are shown as red squares in panels (b) and (c). All overshooting convective tops within +/-3 hours of the red squares are shown by green symbols in panels (b) and (c). Back trajectories from the flight track follow the anticyclonic NAM circulation over Western Mexico, Great Plains and Mississippi Valley (Figure 6b). Every one of the example back trajectories intersects OT, as shown by red symbols in Figure 6b. For this flight, coincidences with overshooting convection are dominated by overshooting clouds over the Mississippi Valley and Great Plains. All overshooting convection within the tolerances prescribed (see Sect. 3.2) for the back trajectories are shown by the green symbols in Figure 6b and 5c. Figure 6c demonstrates the range of altitudes reached by the coincident overshooting convection and how many convective overshooting cells were coincident. The high resolution of the convective overshooting data meant that there could be multiple coincident convective overshooting cells for a single location on a back trajectory. It is significant that some of the green overshooting cells are higher altitude than the red coincident points, suggesting that overshooting air parcels descended slightly before mixing with the surrounding air. Figure 6d indicates the source of enhanced water was dominated by overshooting clouds within seven days prior to intercept by the aircraft.

Deleted: Figure 7

Deleted: Figure 7

Deleted: Figure 7

Deleted: Figure 7

Deleted: Figure 7

Deleted: Figure 7

4.2 Second case: 16 August 2013

The NASA ER-2 flight of 16 August 2013 was designed to survey the North American Monsoon in a triangular flight path from Houston, Texas, to the Imperial Valley in Southern California, to Southeastern Colorado and back to Texas. The NASA ER-2 aircraft performed six dives, encountering enhanced stratospheric water at 16 to 17 km altitude (Figure 7a). As shown in Figure 7b, back trajectories intersect overshooting tops over the South Central U.S. (Texas, Oklahoma, Arkansas) and also over the Sierra Madre Occidental mountain range on the west coast of Mexico. This case is an example of the classic North American Monsoon circulation with a moisture source over the Sierra Madre Occidental (Adams and Comrie, 1997), in which air parcels are transported from OT in Mexico,

Deleted: Figure 8

Deleted: Figure 8

Deleted: .

Deleted: Anticyclonic transport carried the moisture north from Mexico, and counter-clockwise around the high pressure around the anticyclone, to the CONUS (Figure 7b). The altitude range of the convective overshoot is typically 16 to 17 km altitude, as shown in Figure 7c. The time between OT and intercept by the aircraft ranges from two to seven days (Figure 7d).

4.3 Third case: 27 August 2013

The 27 August 2013 flight performed six dives to sample the North American Monsoon. Stratospheric water was enhanced to 15 to 20 ppmv in altitudes ranging from 16.0 to 17.5 km (Figure 8a). The ER-2 aircraft intercepted highly enhanced stratospheric water from a mesoscale convective complex over the Upper Midwest, which had overshooting tops over Northern Minnesota and Northern Wisconsin (Toon et al., 2016), as shown in Figure 8b. Figure 8c shows an abundance of OT above 17 km (green). Generally speaking, the OT appear at higher altitudes in the northern CONUS/southern Canada than in the Central CONUS. Figure 8d shows that the air masses were sampled *in situ* by the ER-2 aircraft over Illinois and Indiana one to two days after the intense storm. As is a common theme for all these experiment days, a portion of the back-trajectories also trace back to overshooting tops over the Sierra Madre Occidental one week prior.

5. Conclusions

In this paper, we have examined *in situ* measurements of stratospheric water by JLH Mark2 on the ER-2 aircraft during the SEAC[4]RS field mission. With JLH Mark2 data, enhanced H_2O above background mixing ratios was frequently encountered in the overworld stratosphere between 16 and 17.5 km altitude. Back trajectories initialized at every 1-sec time stamp along the aircraft flight track at 16 to 17.5 km connect the sampled air parcels to convective OT within seven days prior to the flight. The trajectory modeling indicates that the identified OT are associated with larger storm systems over the Central U.S. (Figure 6), deep convection over the Sierra Madre Occidental (Figure 7), and deep convection over the Upper Midwest U.S. and South Central Canada (Figure 8). For all the back trajectories in the three case studies, the fraction that connect to OT within the previous seven days ranges from 30% to 70% (Figure 9). The three aircraft flight dates analyzed in Figure 9 have a higher fraction of enhanced water than the other flights. These three flights deliberately targeted air masses influenced by convection. For the CONUS in general, the fraction of air parcels at 370-420 K influenced by OT is much smaller.

The concentrations of enhanced water and the connection to OT suggests a mechanism for moistening the CONUS lower stratosphere: ice is irreversibly injected into the overworld stratosphere by the most intense convective tops. The temperatures of the CONUS lower stratosphere are sufficiently warm to sublimate the ice, producing water vapor mixing ratios elevated 10 ppmv or more above background levels. The summertime CONUS has a high frequency of thunderstorms with sufficient energy to transport ice to the upper troposphere (Koshak et al., 2015, and references therein). On rare occasion, these storms have sufficient energy to loft ice through the tropopause and into the stratosphere. Further evidence of ice is provided by water isotopologues. Evaporation and condensation are fractionating processes for isotopologues, especially HDO relative to H_2O (e.g., Craig, 1961; Dansgaard, 1964). Condensation preferentially concentrates the heavier HDO isotopologue, so lofted ice is relatively enriched in

Deleted: Figure 8
Deleted: Figure 8
Deleted: Figure 8
Deleted: Figure 9
Deleted: Figure 9
Deleted: Figure 9
Deleted: Figure 9
Deleted: initialized
Deleted: Figure 7
Deleted: Figure 8
Deleted: Figure 9
Deleted: this analysis
Deleted: Figure 10

HDO/H_2O compared to gas phase (e.g., Webster and Heymsfield, 2003, and references therein). Ice sublimation is supported by the enriched HDO/H_2O isotopic signature observed by the ACE satellite over summertime North America (Randel et al., 2010). Cross-tropopause transport is a consequence of turbulent mixing at cloud top, possibly enhanced by the existence of breaking gravity waves often occurring near overshooting cloud tops. (Wang, 2003). This study addresses a primary goal of the SEAC^{4}RS field mission (Toon et al., 2016), answering affirmatively the science question: "Do deep convective cloud systems locally inject water vapor and other chemicals into the overworld stratosphere over the CONUS?" This water is almost certainly injected in the ice phase and subsequently sublimated in the relatively warm stratosphere over CONUS, leading to irreversible hydration. From this study, we conclude that the depth of injection was typically 16 to 17.5 km altitude for these particular summertime events.

Satellite retrievals of water vapor from Aura MLS provide a larger-scale context. The fraction of Aura MLS observations at 100 hPa (approximately 17 km altitude) with H_2O greater than the 8 ppmv threshold is 0.9% for July-August 2013. In comparison, Schwartz et al. (2013) reports that, for the nine-year record 2004-2012, July and August had 1.4% and 3.2% of observations exceed 8 ppmv, respectively. This reinforces the conclusion of Randel et al. (2015) that OT play a minor role in the mid-latitude stratospheric water budget. At the 100-hPa level in the lower stratosphere, the year 2013 was slightly drier than the average of 2004-2012 summers (Figure 3). Despite the relatively dry conditions of summer 2013, there was sufficient enhanced water to be clearly observed in the Aura MLS retrievals (Figures 3, 4, 5). Limb measurements from Aura MLS come from a ~200 km path through the atmosphere with ~3 km vertical resolution in the lower stratosphere (Livesey et al., 2016). The aircraft profiles of water vapor are very similar on ascent and descent profiling (Figure 5c), which allows us to estimate the horizontal length of these features as greater than 180 km, and a vertical thickness of ~0.5 km. This size is sufficiently large that the MLS retrieval is sensitive to enhanced water, as shown in Figure 5c.

Deleted: Figure 4

Deleted: , 6

Deleted: Figure 6

Deleted: Figure 6

In situ measurements probe on a small-scale air parcels that can be connected to OT that inject ice and, to a lesser extent, trace gases to the stratosphere (e.g., Ray et al., 2004; Hanisco et al., 2007; Jost et al, 2004). In contrast, modeling studies tend to focus on large-scale processes. Dessler et al. (2002) and Corti et al. (2008) concluded that OT are a significant source of water vapor in the mid-latitude lower stratosphere. In contrast, Randel et al. (2015) used Aura MLS observations to conclude that circulation plays a larger role than OT in controlling mid-latitude stratospheric water vapor in the NAM monsoon region. Our study shows clear evidence of observable perturbations to stratospheric water vapor on ER-2 aircraft flights that targeted convectively-influenced air during SEAC^{4}RS. In future work, we plan more detailed back trajectory analysis of air parcels over summertime North America to better understand the transport of ice and water in the lower stratosphere.

Code Availability

n/a

Data Availability

Data discussed in this manuscript are publically available. The NASA aircraft data are available through the following digital object identifier (DOI): SEAC4RS DOI 10.5067/Aircraft/SEAC4RS/Aerosol-TraceGas-Cloud.

Appendices: none

Supplement link: none

Team List:

Robert L. Herman[1], Eric A. Ray[2], Karen H. Rosenlof[2], Kristopher M. Bedka[3], Michael J. Schwartz[1], William G. Read[1], Robert F. Troy[1], Keith Chin[1], Lance E. Christensen[1], Dejian Fu[1], Robert A. Stachnik[1], T. Paul Bui[4], Jonathan M. Dean-Day[5]

[1]Jet Propulsion Laboratory, California Institute of Technology, Pasadena, California, USA.

[2]National Oceanic and Atmospheric Administration (NOAA) Earth System Research Laboratory (ESRL) Chemical Sciences Division, Boulder, Colorado, USA.

[3]NASA Langley Research Center, Hampton, Virginia, USA.

[4]NASA Ames Research Center, Moffett Field, California, USA.

[5]Bay Area Environmental Research Institute, Sonoma, California, USA.

Author Contribution

Robert Herman prepared the manuscript with contributions from all coauthors and was responsible for all aspects of the JLH Mark2 as principal investigator. Eric Ray and Karen Rosenlof provided trajectory calculations and interpretation. Kristopher Bedka provided an overshooting top data product and interpretation. Robert Troy, Robert Stachnik and Keith Chin operated the JLH Mark2 instrument in the field and downloaded data. Robert Stachnik, Dejian Fu, Lance Christensen and Keith Chin also developed software components for the JLH Mark2 instrument. Michael Schwartz and William Read provided Aura MLS data and statistical analysis. T. Paul Bui and Jonathan Dean-Day measured pressure and temperature with the MMS instrument and provided data.

Competing interests:

The authors declare that they have no conflict of interest.

Disclaimer

Acknowledgements

We thank Jose Landeros and Dave Natzic for providing technical support in the laboratory and field, and the aircraft crew and flight planners for making these measurements possible. The JLH Mark2 team is supported by the NASA Upper Atmosphere Research Program and Radiation Sciences Program. Part of this research was performed at JPL, California Institute of Technology, under a contract with NASA.

References

Adams, D. K., and A. C. Comrie: The North American Monsoon. *Bull. Amer. Meteor. Soc.*, 78, 2197–2213, doi:http://dx.doi.org/10.1175/JCLI4071.1, 1997.

Anderson, J. G., Wilmouth, D. M., Smith, J. B., and Sayres, D. S.: UV Dosage Levels in Summer: Increased Risk of Ozone Loss from Convectively Injected Water Vapor, *Science*, 337(6096), 835-839, 2012.

Bedka, K. M., Brunner, J., Dworak, R., Feltz, W., Otkin, J., and Greenwald, T.: Objective satellite-based overshooting top detection using infrared window channel brightness temperature gradients. *J. Appl. Meteor. Climatol.*, **49**, 181-202, 2010.

Bedka, K. M., Wang, C., Rogers, R., Carey, L., Feltz, W., and Kanak, J.: Examining deep convective cloud evolution using total lightning, WSR-88D, and GOES-14 super rapid scan datasets, *Wea. Forecasting*, 30, 571–590, doi:10.1175/WAF-D-14-00062.1, 2015.

Boucher, O., Randall, D., Artaxo, P., Bretherton, C., Feingold, G., Forster, P., Kerminen, V.-M., Kondo, Y., Liao, H., Lohmann, U., Rasch, P., Satheesh, S. K., Sherwood, S., Stevens B., and Zhang, X. Y.: Clouds and Aerosols. In: Climate Change 2013: The Physical Science Basis. Contribution of Working Group I to the Fifth Assessment Report of the Intergovernmental Panel on Climate Change (Stocker, T. F., Qin, D., Plattner, G.-K., Tignor, M., Allen, S. K., Boschung, J., Nauels, A., Xia, Y., Bex, V., and Midgley, P. M. (eds.)), Cambridge University Press, Cambridge, United Kingdom and New York, NY, USA, 2013.

Brewer, A. W.: Evidence for a world circulation provided by the measurements of helium and water vapor distribution in the stratosphere, *Q. J. Roy. Met. Soc.,* 75, 351-63, 1949.

Corti, T., Luo, B. P., De Reus, M., Brunner, D., Cairo, F., Mahoney, M. J., Martucci, G., Matthey, R., Mitev, V., Dos Sntos, F. H., Schiller, C., Shur, G., Sitnikov, N. M., Spelten, N., Voessing, H. J., Borrmann, S., and Peter, T.: Unprecedented evidence for deep convection hydrating the tropical stratosphere, *Geophys. Res. Lett., 35,* L10810, doi:10.1029/2008GL033641, 2008.

Craig, H.: Isotopic Variations in Meteoric Waters, *Science, 133,* 1702-3, doi: 10.1126/science.133.3465.1702, 1961.

Dansgaard, W.: Stable isotopes in precipitation, *Tellus, 16,* 436-68, 1964.

Dessler, A. E., Hanisco, T. F, and Fueglistaler, S.: Effects of convective ice lofting on H_2O and HDO in the tropical tropopause layer, *J. Geophys. Res., 112*, doi:10.1029/2007JD008609, 2007.

Fahey, D. W., Gao, R.-S., Möhler, O., Saathoff, H., Schiller, C., Ebert, V., Krämer, M., Peter, T., Amarouche, N., Avallone, L. M., Bauer, R., Bozóki, Z., Christensen, L. E., Davis, S. M., Durry, G., Dyroff, C., Herman, R. L., Hunsmann, S., Khaykin, S., Mackrodt, P., Meyer, J., Smith, J. B., Spelten, N., Troy, R. F., Vömel, H., Wagner, S., and Weinhold, F. G.: The AquaVIT-1 Intercomparison of Atmospheric Water Vapor Measurement Techniques, Atmos. Meas. Tech., 7, 3177-3213, doi:10.5194/amt-7-3177-2014, 2014.

Flury, T., Wu, D. L., and Read, W. G.: Variability in the speed of the Brewer-Dobson circulation as observed by Aura/MLS, *Atmos. Chem. Phys., 13,* 4563–4575, www.atmos-chem-phys.net/13/4563/2013/, doi:10.5194/acp-13-4563-2013, 2013.

Griffin, S. M., Velden, C. S., and Bedka, K. M.: A method for calculating the height of overshooting convective cloud tops using satellite-based IR imager and CloudSat cloud profiling radar observations, J. Appl. Met. and Clim., 55, 479-491, DOI: http://dx.doi.org/10.1175/JAMC-D-15-0170.1, 2016.

Hanisco, T. F., Moyer, E. J., Weinstock, E. M., St. Clair, J. M., Sayres, D. S., Smith, J. B., Lockwood, R., Anderson, J. G., Dessler, A. E., Keutsch, F. N., Spackman, J. R., Read, W. G., and Bui, T. P.: Observations of deep convective influence on stratospheric water vapor and its isotopic composition, *Geophys. Res. Lett., 34,* L04814, doi:10.1029/2006GL027899, 2007.

Holton, J.R., P.H. Haynes, A.R. Douglass, R.B. Rood, and L. Pfister: Stratosphere–troposphere exchange. Rev. Geophys., 33(4), 403–439, 1995.

Homeyer, C., McAuliffe, J., and Bedka, K. M.: On the Development of Above-Anvil Cirrus Plumes in Extratropical Convection, *J. Atmos. Sci.*, In Press, available online at: http://journals.ametsoc.org/doi/abs/10.1175/JAS-D-16-0269.1

Jensen, E. J., Diskin, G., Lawson, R. P., Lance, S., Bui, T. P., Hlavka, D., McGill, M., Pfister, L., Toon, O. B., and Gao, R., Ice nucleation and dehydration in the Tropical Tropopause Layer, Proc. Nat. Acad. Sci., 110(6), 2041–2046, 2013.

Jensen, E. J., Smith, J. B., Pfister, L., Pittman, J. V., Weinstock, E. M., Sayres, D. S., Herman, R. L., Troy, R. F., Rosenlof, K., Thompson, T. L., Fridlind, A. M., Hudson, P. K., Cziczo, D. J., Heymsfield, A. J., Schmitt, C. and Wilson, J. C.: Ice Supersaturations Exceeding 100% at the Cold Tropical Tropopause: Implications for Cirrus Formation and Dehydration, Atmos. Chem. Phys., 5, 851-62, 2005.

Jost, H. J., et al.: In-situ observations of mid-latitude forest fire plumes deep in the stratosphere, Geophys. Res. Lett., 31, L11101, doi:10.1020/2003GL019253, 2004.

Kirk-Davidoff, D. B., Hintsa, E. J., Anderson, J. G., and Keith, D. W.: The effect of climate change on ozone depletion through changes in stratospheric water vapour, *Nature, 402*, 399-401, doi:10.1038/46521, 1999.

Koshak, W. J., Cummins, K. L., Buechler, D. E., Vant-Hull B., Blakeslee, R. J., Williams, E. R., and H. S. Peterson: Variability of CONUS Lightning in 2003-12 and Associated Impacts, *J. Appl. Meteor. Climat., 54*, 15-41,doi:10.1175/JAMC-D-14-0072.1, 2015.

Livesey, N. J., Read, W. G., Wagner, P. A., Froidevaux, L., Lambert, A., Manney, G. L., Millan Valle, L. F., Pumphrey, H. C., Santee, M. L., Schwartz, M. J., Wang, S., Fuller, R. A., Jarnot, R. F., Knosp, B. W., and Martinez, E.: Earth Observing System (EOS) Aura Microwave Limb Sounder (MLS) Version 4.2x Level 2 data quality and description document, Tech. Rep. JPL D-33509 Rev. B, Version 4.2x-2.0, Jet Propulsion Laboratory, California Institute of Technology, Pasadena, CA, available online at: http://mls.jpl.nasa.gov/data/datadocs.php (last access: May 9, 2016), 2016.

Liu, C., Zipser, E. J., Cecil, D. J., Nesbitt, S. W., Sherwood, S.: *J. Appl. Meteorol. Climatol. 47*, 2712: 2008.

Liu, N., and Liu, C.: Global distribution of deep convection reaching tropopause in 1 year GPM observations, *J. Geophys. Res. Atmos., 121,* doi:10.1002/2015JD024430, 2016.

May, R. D.: Open-path, near-infrared tunable diode laser spectrometer for atmospheric measurements of H_2O, J. Geophys. Res., 103(D15), 19161-19172, doi:10.1029/98jd01678, 1998.

Moyer, E., Irion, F., Yung, Y., and Gunson, M.: ATMOS stratospheric deuterated water and implications for troposphere-stratosphere transport, *Geophys. Res. Lett., 23*(17), 2385-88, 1996.

Mullendore, G. L., Durran, D. R., and Holton, J. R.: Cross-tropopause tracer transport in midlatitude convection, *J. Geophys. Res., 110,* D06113, doi:10.1029/2004JD005059, 2005.

Mullendore, G. L., Homann, A. J., Bevers, K., and Schumacher, C.: Radar reflectivity as a proxy for convective mass transport*, J. Geophys. Res., 114,* D16103, doi:10.1029/2008JD011431, 2009.

Randel, W. J., K. Zhang, and R. Fu: What controls stratospheric water vapor in the NH summer monsoon regions?, *J. Geophys. Res.*, 120, 7988–8001, doi:10.1002/2015JD023622, 2015.

Ravishankara, A. R.: Water Vapor in the Lower Stratosphere, Science, 337, 809–810, doi: 10.1126/science.1227004, 2012.

Ray, E. A., Rosenlof, K. H., Richard, E. C., Hudson, P. K., Cziczo, D. J., Loewenstein, M., Jost, H.-J., Lopez, J., Ridley, B., Weinheimer, A., Montzka, D., Knapp, D., Wofsy, S. C., Daube, B. C., Gerbig, C., Xueref, I., and Herman, R. L.: Evidence of the effect of summertime midlatitude convection on the subtropical lower stratosphere from CRYSTAL-FACE tracer measurements, J. Geophys. Res., 109(D18), D18304, doi: 10.1029/2004JD004655, 2004.

Read, W. G., et al.: Aura Microwave Limb Sounder upper tropospheric and lower stratospheric H_2O and relative humidity with respect to ice validation, J. Geophys. Res. Atmospheres, 112(D24), D24S35, doi:10.1029/2007jd008752, 2007.

Roach, W. T.: On the nature of the summit areas of severe storms in Oklahoma, *Q. J. R. Meteorol. Soc., 93*, 318–336, 1967.

Rodgers, C. D.: Inverse Methods for Atmospheric Sounding: Theory and Practice, World Science, London, 2000.

Rodgers, C. D., and Connor, B. J.: Intercomparison of Remote Sounding Instruments, J. Geophys. Res., 108, 4116, doi: 10.1029/2002JD002299, 2003.

Rollins, A., Thornberry, T., Gao, R. S., Smith, J. B., Sayres, D. S., Sargent, M. R., Schiller, C., Krämer, M., Spelten, N., Hurst, D. F., Jordan, A. F., Hall, E. G., Vömel, H., Diskin, G. S., Podolske, J. R., Christensen, L. E., Rosenlof, K. H., Jensen, E. J., and Fahey, D. W.: Evaluation of UT/LS hygrometer accuracy by inter-comparison during the NASA MACPEX mission, J. Geophys. Res.-Atmos., 119, doi:10.1002/2013JD020817, 2014.

Saha, S. et al.: The NCEP Climate Forecast System Version 2, J. Climate, 27, 2185–2208, doi:10.1175/JCLI-D-12-00823.1, 2014.

Sargent, M. R., Smith, J. B., Sayres, D. S., and Anderson, J. G.: The roles of deep convection and extratropical mixing in the Tropical Tropopause Layer: An in situ measurement perspective, *J. Geophys. Res., 119*(21), 12355-71, DOI:10.1002/2014JD022157, 2014.

Sayres, D. S., Pfister, L., Hanisco, T. F., Moyer, E. J., Smith, J. B., St. Clair, J. M., O'Brien, A. S., Witinski, M. F., Legg, M., and Anderson, J. G.: Influence of convection on the water isotopic composition of the tropical tropopause layer and tropical stratosphere, *J. Geophys. Res., 115,* D00J20, doi:10.1029/2009JD013100, 2010.

Schwartz, M. J., Read, W. G., Santee, M. L., Livesey, N. J., Froidevaux, L., Lambert, A., and Manney, G. L.: Convectively injected water vapor in the North American summer lowermost stratosphere, Geophys. Res. Lett., 40, 2316-2321, doi:10.1002/grl.50421, 2013.

Scott, S. G., Bui, T. P., Chan, K. R., and Bowen, S. W.: The meteorological measurement system on the NASA ER-2 aircraft, J. Atmos. Ocean. Tech., 7, 525-40, 1990.

Shindell, D. T.: Climate and ozone response to increased stratospheric water vapor, *Geophys. Res. Lett., 28,* 1551-4, 2001.

Smith, J. B., Sargent, M., Wilmouth, D. and Anderson, J. G.: Quantifying the Direct Convective Transport of Tropospheric Air to the Overworld Statosphere, Abstract A51O-0288, presented at 2015, Fall Meeting, AGU, San Francisco, CA, 14-18 December, 2015.

Solomon, D. L., Bowman, K. P., and Homeyer, C. R.: Tropopause-Penetrating Convection from Three-Dimensional Gridded NEXRAD Data, *J. Appl. Met. Climat., 55,* 465-78, DOI:10.1175/JAMC-D-15-0190.1, 2016.

Solomon, S., Rosenlof, K. H., Portmann, R. W., Daniel, J. S., Davis, S. M., Sanford, T. J., and Plattner, G.-K.: Contributions of Stratospheric Water Vapor to Decadal Changes in the Rate of Global Warming, Science, 327(5970), 1219-1223, doi:10.1126/science.1182488, 2010.

Stohl, A., C. Forster, A. Frank, P. Seibert, and G. Wotawa: Technical note: The Lagrangian particle dispersion model FLEXPART version 6.2, Atmos. Chem. Phys., 5, 2461-2474, doi: 10.5194/acp-5-2461-2005-supplement, 2005.

Toon, O. B., H. Maring, J. Dibb, R. Ferrare, D. J. Jacob, E. J. Jensen, Z. J. Luo, G. G. Mace, L. L. Pan, L. Pfister, K. H. Rosenlof, J. Redemann, J. S. Reid, H. B. Singh, A. M. Thompson, R. Yokelson, P. Minnis, G. Chen, K. W. Jucks, and A. Pszenny: Planning, implementation and scientific goals of the Studies of Emissions and Atmospheric Composition, Clouds and Climate Coupling by Regional Surveys (SEAC^{4}RS) field mission, *J. Geophys. Res., 121*, 4967-5009, doi:10.1002/2015JD024297, 2016.

Voemel, H., et al.: Balloon-borne observations of water vapor and ozone in the tropical upper troposphere and lower stratosphere, *J. Geophys. Res.*, 107(D14), pages ACL 8-1-ACL 8-16, DOI:10.1029/2001JD000707, 2002. Available online at http://onlinelibrary.wiley.com/doi/10.1029/2001JD000707/full#jgrd8979-fig-0017, 2002.

Wang, P. K., Moisture plumes above thunderstorm anvils and their contributions to cross-tropopause transport of water vapor in midlatitudes, *J. Geophys. Res., 108*(D6), 4194, doi:10.1029/2002JD002581, 2003.

Webster, C. R., and Heymsfield, A. J.: Water Isotope Ratios D/H, $^{18}O/^{16}O$, $^{17}O/^{16}O$ in and out of Clouds Map Dehydration Pathways, *Science*, 302, 1742, DOI: 10.1126/science.1089496, 2003.

TABLES

Table 1 Summary of enhanced water vapor measurements in the overworld stratosphere during SEAC[4]RS*. Dates are NASA ER-2 aircraft flight dates in day-month-year format, and JLH Mark2 maximum water vapor mixing ratios (ppmv) are shown for potential temperatures greater than 400 K (left) and in the range 380-400 K (right).

Date	max. water (ppmv)	Pot. Temp. (K)	Altitude (km)	max. water (ppmv)	Pot. Temp. (K)	Altitude (km)
	above 400 K	above 400 K	above 400 K	380-400K	380-400K	380-400K
8-Aug-2013	10.1	401.2	17.29	11.2	385.7	17.10
12-Aug-2013	8.0	400.1	17.08	13.2	388.1	16.86
14-Aug-2013	7.7	402.2	17.38	10.7	387.4	16.75
16-Aug-2013	7.0	400.2	17.14	12.2	387.3	16.82
27-Aug-2013	15.3	402.8	17.32	17.7	380.8	16.12
30-Aug-2013	9.2	400.2	17.27	12.0	390.0	16.81
2-Sep-2013	8.0	400.3	17.07	13.0	380.3	16.28
4-Sep-2013	6.3	405.0	17.57	10.8	380.2	16.32
6-Sep-2013	6.8	400.1	17.12	15.6	381.0	16.32
11-Sep-2013	7.7	400.2	17.13	10.2	381.0	16.22
13-Sep-2013	6.9	401.8	17.55	9.2	382.4	16.41

* SEAC[4]RS = Studies of Emissions and Atmospheric Composition, Clouds and Climate Coupling by Regional Surveys

FIGURE CAPTIONS

Figure 1. JLH Mark2 stratospheric water vapor profiles from 23 aircraft flights during SEAC[4]RS. This altitude range includes the overworld stratosphere (potential temperature greater than 380 K) and lowermost stratosphere (tropopause to 380 K). The majority of observations have mixing ratios less than 10 ppmv in the lowermost stratosphere and less than 6 ppmv in the overworld stratosphere. Enhanced water measurements are the extreme outliers with high water mixing ratios, with a threshold value of mean plus two standard deviations.

Figure 2. Distribution of JLH Mark2 water vapor in the overworld stratosphere for all flights in the SEAC[4]RS mission (summer 2013), plotted as fraction of observations in each potential temperature range. First trace (black circles and line) is at potential temperatures 380 K to 400 K corresponding to approximately 16.8 to 17.4 km altitude (99 to 90 hPa). Second trace (red triangles and line) is at potential temperatures 400 to 420 K corresponding to approximately 17.4 to 18.0 km altitude (90 to 80 hPa).

Figure 3. Distribution of Aura MLS v4.2 100-hPa H_2O over CONUS (blue shaded box in insert), corresponding to approximately 17 km altitude. The two histograms for July-August 2013 (blue asterisks and trace) and the previous nine-summer MLS record, July-August 2004 through 2012 (red circles and trace) indicates that 2013 was drier than average. The threshold for MLS-detected 'enhanced water vapor' (thick black vertical line) is set at 8 ppmv, same as Schwartz et al. (2013), to exclude the larger population of measurements at 6 to 8 ppmv water vapor that may have other sources.

Deleted: Distribution of JLH Mark2 water vapor at potential temperatures 380 K to 400 K in the overworld stratosphere for all flights in the SEAC[4]RS mission (summer 2013). These potential temperatures correspond to approximately 16.8 to 17.4 km altitude (99 to 90 hPa).

Deleted: Figure 4

Deleted: Figure 4

Figure 4. Two-month mean map of Aura MLS v4.2 100-hPa H_2O (color scale), corresponding to approximately 17 km altitude, with superimposed MERRA horizontal winds (arrows) for July-August 2013 during the SEAC^{4}RS time period. MLS observations of 100-hPa H_2O greater than 8 ppmv in this two-month period are shown by the white circles.

Deleted: Figure 5

Figure 5. Map and profiles of aircraft and satellite water vapor on 8 August 2013 over California (number 1 shown in dark blue) and Texas (number 2 shown in green). (a) Map of ER-2 aircraft flight track (solid colored trace) and nearly coincident Aura MLS geolocations (asterisks and lines). (b) ER-2 aircraft altitude profiles (solid colored trace) color-coded by dives and MLS times (horizontal lines). (c) Vertical profiles of *in situ* water vapor measurements from JLH Mark2 (dots) and MLS retrievals of water vapor (circles and lines). Some measurements exceed the threshold for enhanced water vapor of 8 ppmv for Aura MLS (after Schwartz et al., 2013), and the campaign-wide mean plus 2 st. dev. for JLH Mark 2, 9.7 ppmv at 380-400 K and 6.6 ppmv at 400-420 K.

Deleted: Figure 6

Figure 6. Analysis of the 8 August 2013 NASA ER-2 aircraft flight. (a) Vertical profiles of JLH Mark2 *in situ* H_2O. Back trajectories were initialized from all aircraft water measurements at 16 to 17.5 km altitude. (b) Example back trajectories (thin blue traces) and coincident overshooting convection (red). Along the NASA ER-2 flight track (orange line), enhanced water vapor was measured (thick blue lines). This figure identifies where trajectories and OT are coincident (red squares) within tolerances prescribed in Section 3.2. The green markers are overshooting convective tops within +/-3 hours of the red squares to indicate the main regions of convective overshooting during the seven days prior to the ER-2 flight and which of those regions appeared to contribute most to the water vapor enhancement measured on the flight. (c) Altitude plot of example back trajectories showing coincident overshooting (red squares). The green markers are overshooting convective tops within +/-3 hours of the red squares. The high resolution of the convective overshooting data meant that there could be multiple coincident convective overshooting cells for a single location on a back trajectory, (d) Days between OT and intercept by aircraft on 8 August 2013.

Deleted: Figure 7

Figure 7. Analysis of the 16 August 2013 NASA ER-2 flight. (a) Vertical profiles of JLH Mark2 *in situ* H_2O similar to Figure 6a, (b) Back trajectories from the aircraft path similar to Figure 6b, (c) Altitude plot of back trajectories showing coincident overshooting (red) and all overshooting within +/- 3 hours (green) similar to Figure 6c, (d) Days between OT and intercept by aircraft similar to Figure 6d.

Deleted: Figure 8

Deleted: Figure 7

Deleted: Figure 7

Deleted: Figure 7

Deleted: Figure 7

Figure 8. Analysis of the 27 August 2013 NASA ER-2 flight. (a) Vertical profiles of JLH Mark2 *in situ* H_2O similar to Figure 6a, (b) Back trajectories from the aircraft path similar to Figure 6b, (c) Altitude plot of back trajectories showing coincident overshooting (red) and all overshooting within +/- 3 hours (green) similar to Figure 6c, (d) Days between OT and intercept by aircraft similar to Figure 6d.

Deleted: Figure 9

Deleted: Figure 7

Deleted: Figure 7

Deleted: Figure 7

Deleted: Figure 7

Figure 9. Fraction of back trajectories that intersected OTs during the 7 previous days for the three SEAC^{4}RS flights of 8 August (blue), 16 August (green) and 27 August 2013 (red) shown in Figures 6, 7 and 8, respectively.

Deleted: Figure 10

Deleted: 7

Deleted: 8

Deleted: 9

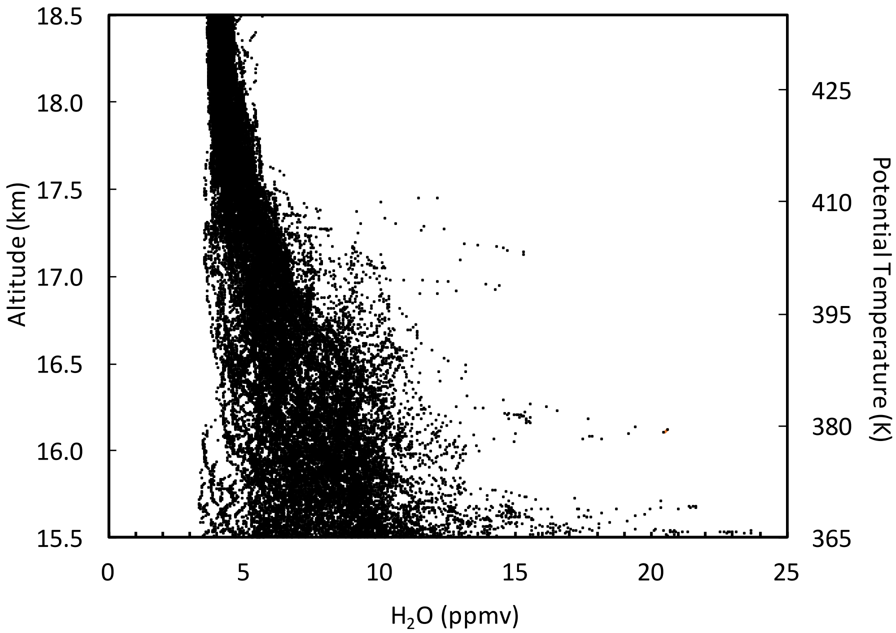

Figure 1. JLH Mark2 stratospheric water vapor profiles from 23 aircraft flights during SEAC[4]RS. This altitude range includes the overworld stratosphere (potential temperature greater than 380 K) and lowermost stratosphere (tropopause to 380 K). The majority of observations have mixing ratios less than 10 ppmv in the lowermost stratosphere and less than 6 ppmv in the overworld stratosphere. Enhanced water measurements are the extreme outliers with high water mixing ratios, with a threshold value of mean plus two standard deviations.

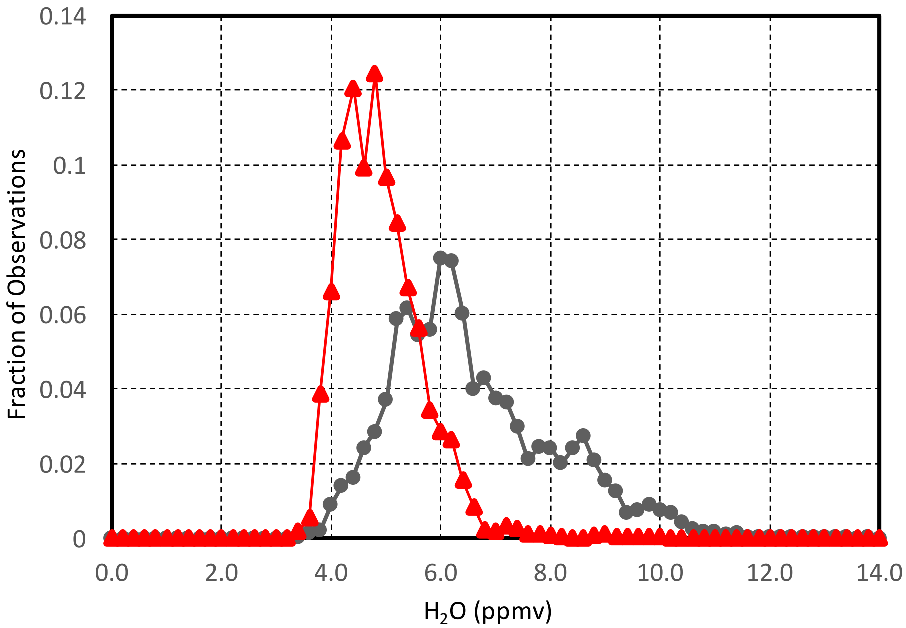

Figure 2. Distribution of JLH Mark2 water vapor in the overworld stratosphere for all flights in the SEAC^{4}RS mission (summer 2013), plotted as fraction of observations in each potential temperature range. First trace (black circles and line) is at potential temperatures 380 K to 400 K corresponding to approximately 16.8 to 17.4 km altitude (99 to 90 hPa). Second trace (red triangles and line) is at potential temperatures 400 to 420 K corresponding to approximately 17.4 to 18.0 km altitude (90 to 80 hPa).

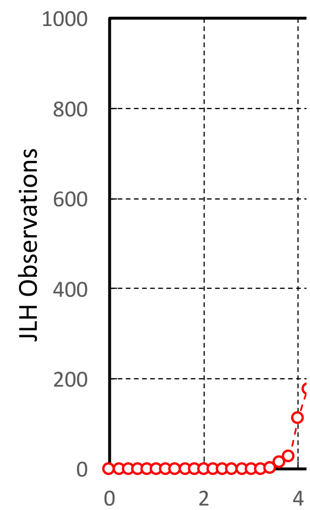

Deleted:

Formatted: Font:(Default) Times New Roman, 10 pt, Bold

Deleted: at potential temperatures 380 K to 400 K

Formatted: Line spacing: 1.5 lines

Deleted: These potential temperatures

Deleted:

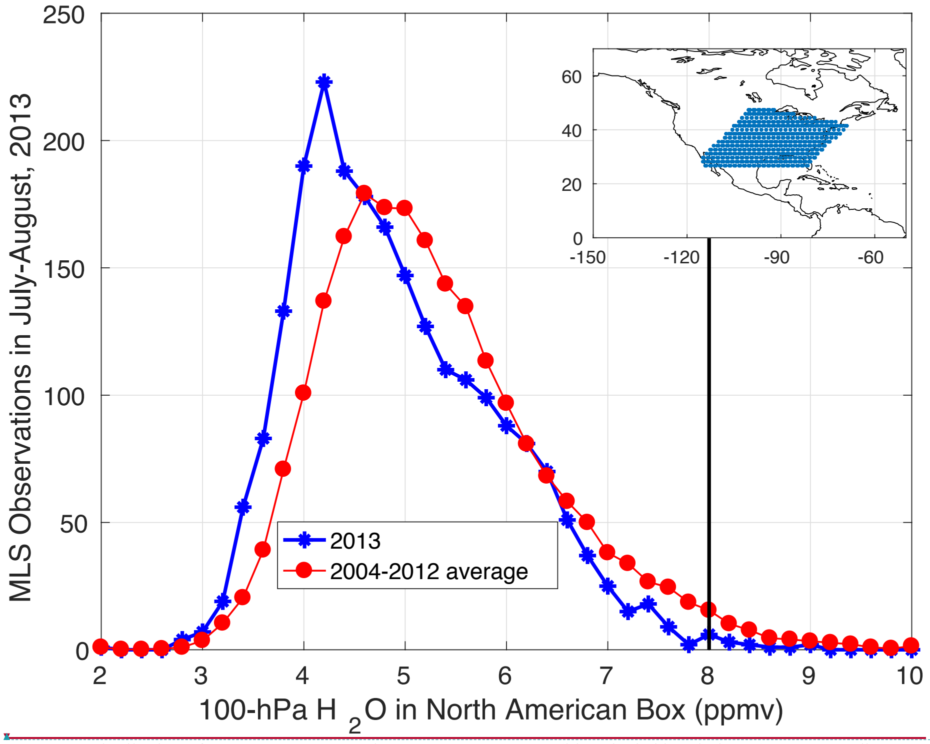

Figure 3. Distribution of Aura MLS v4.2 100-hPa H_2O over CONUS (blue shaded box in insert), corresponding to approximately 17 km altitude. The two histograms for July-August 2013 (blue asterisks and trace) and the previous nine-summer MLS record, July-August 2004 through 2012 (red circles and trace) indicates that 2013 was drier than average. The threshold for MLS-detected ‘enhanced water vapor’ (thick black vertical line) is set at 8 ppmv, same as Schwartz et al. (2013), to exclude the larger population of measurements at 6 to 8 ppmv water vapor that may have other sources.

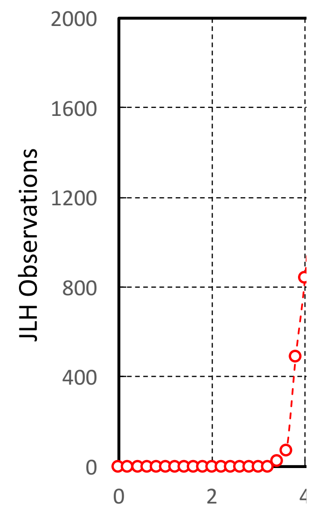

Deleted: Figure 4

Formatted: Font:(Default) Times New Roman, 10 pt, Bold

Formatted: Font:(Default) Times New Roman, 12 pt, Bold

Deleted: Figure 4

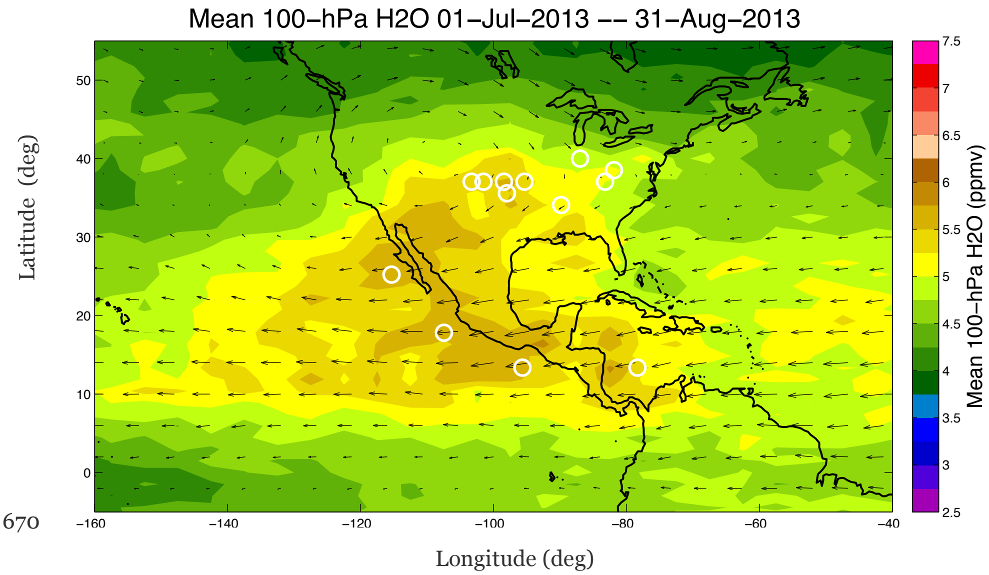

Figure 4. Two-month mean map of Aura MLS v4.2 100-hPa H_2O (color scale), corresponding to approximately 17 km altitude, with superimposed MERRA horizontal winds (arrows) for July-August 2013 during the SEAC[4]RS time period. MLS observations of 100-hPa H_2O greater than 8 ppmv in this two-month period are shown by the white circles.

Deleted: Figure 5

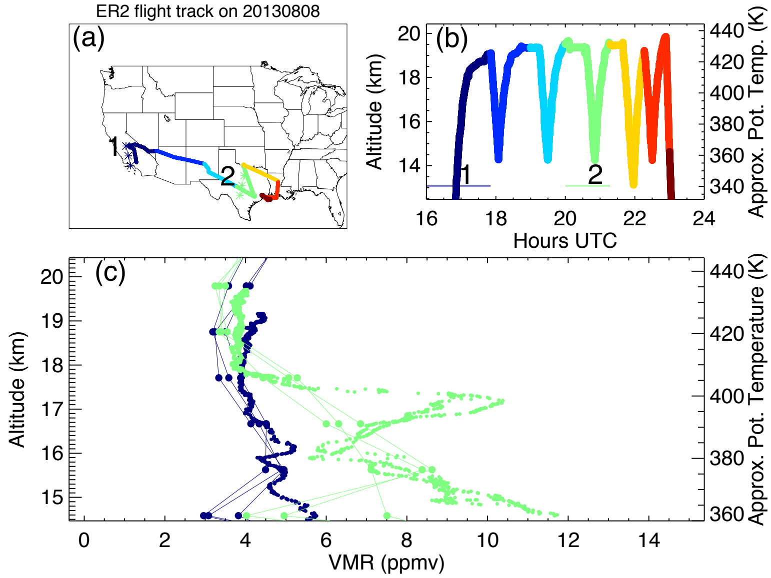

Figure 5. Map and profiles of aircraft and satellite water vapor on 8 August 2013 over California (number 1 shown in dark blue) and Texas (number 2 shown in green). (a) Map of ER-2 aircraft flight track (solid colored trace) and nearly coincident Aura MLS geolocations (asterisks and lines). (b) ER-2 aircraft altitude profiles (solid colored trace) color-coded by dives and MLS times (horizontal lines). (c) Vertical profiles of *in situ* water vapor measurements from JLH Mark2 (dots) and MLS retrievals of water vapor (circles and lines). Some measurements exceed the threshold for enhanced water vapor of 8 ppmv for Aura MLS (after Schwartz et al., 2013), and the campaign-wide mean plus 2 st. dev. for JLH Mark 2, 9.7 ppmv at 380-400 K and 6.6 ppmv at 400-420 K.

Deleted: Figure 6

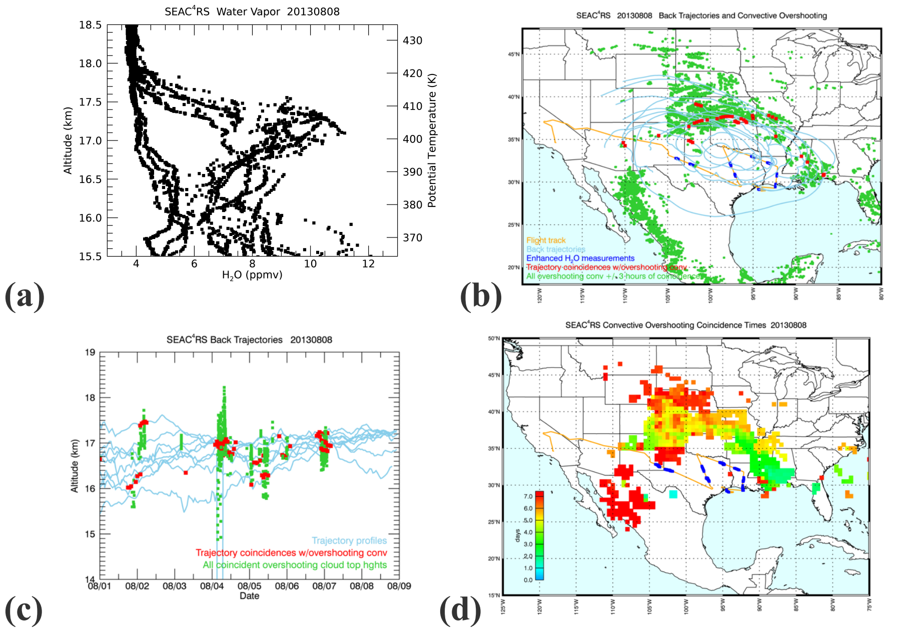

Figure 6. Analysis of the 8 August 2013 NASA ER-2 aircraft flight. (a) Vertical profiles of JLH Mark2 *in situ* H_2O. Back trajectories were initialized from all aircraft water measurements at 16 to 17.5 km altitude. (b) Example back trajectories (thin blue traces) and coincident overshooting convection (red). Along the NASA ER-2 flight track (orange line), enhanced water vapor was measured (thick blue lines). This figure identifies where trajectories and OT are coincident (red squares) within tolerances prescribed in Section 3.2. The green markers are overshooting convective tops within +/-3 hours of the red squares to indicate the main regions of convective overshooting during the seven days prior to the ER-2 flight and which of those regions appeared to contribute most to the water vapor enhancement measured on the flight. (c) Altitude plot of example back trajectories showing coincident overshooting (red squares). The green markers are overshooting convective tops within +/-3 hours of the red squares. The high resolution of the convective overshooting data meant that there could be multiple coincident convective overshooting cells for a single location on a back trajectory, (d) Days between OT and intercept by aircraft on 8 August 2013.

Deleted: Figure 7

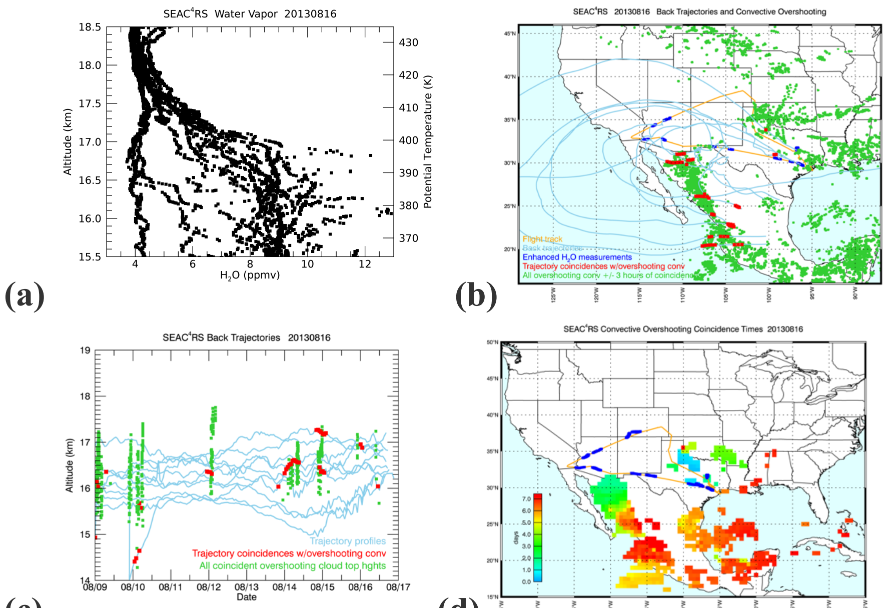

Figure 7. Analysis of the 16 August 2013 NASA ER-2 flight. (a) Vertical profiles of JLH Mark2 *in situ* H_2O similar to Figure 6a, (b) Back trajectories from the aircraft path similar to Figure 6b, (c) Altitude plot of back trajectories showing coincident overshooting (red) and all overshooting within +/- 3 hours (green) similar to Figure 6c, (d) Days between OT and intercept by aircraft similar to Figure 6d.

Deleted: Figure 8

Deleted: Figure 7

Deleted: Figure 7

Deleted: Figure 7

Deleted: Figure 7

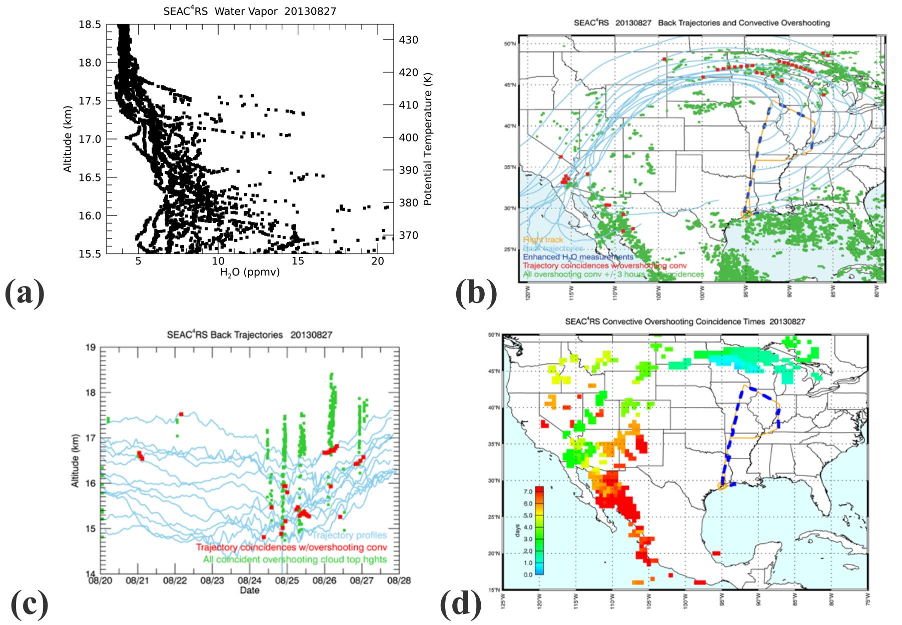

Figure 8. Analysis of the 27 August 2013 NASA ER-2 flight. (a) Vertical profiles of JLH Mark2 *in situ* H_2O similar to Figure 6a, (b) Back trajectories from the aircraft path similar to Figure 6b, (c) Altitude plot of back trajectories showing coincident overshooting (red) and and all overshooting within +/- 3 hours (green) similar to Figure 6c, (d) Days between OT and intercept by aircraft similar to Figure 6d.

Deleted: **Figure 9**

Deleted: Figure 7

Deleted: Figure 7

Deleted: Figure 7

Deleted: Figure 7

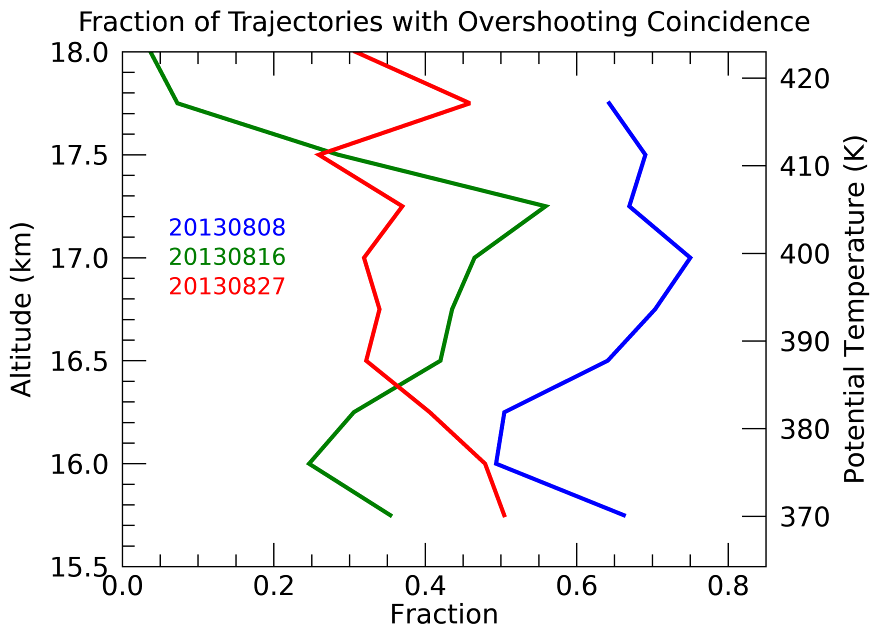

Figure 9. Fraction of back trajectories that intersected OTs during the 7 previous days for the three SEAC[4]RS flights of 8 August (blue), 16 August (green) and 27 August 2013 (red) shown in Figures 6, 7 and 8, respectively.

Deleted: Figure 10

Deleted: 7

Deleted: 8

Deleted: 9